Extending Hollow Cathode Life for Electric Propulsion in Long-Term Missions

Dan M. Goebel[*], Ira Katz[†], James Polk[‡], Ioannis G. Mikellides[§], Kristina K. Jameson[**], Thomas Liu[††]
Jet Propulsion Laboratory, California Institute of Technology, Pasadena, CA 91109

Hollow cathodes are a critical component for the life and performance of most electrostatic and Hall effect ion thrusters. The benchmark life test of a hollow cathode was the Space Station plasma contactor test run at NASA/GRC, in which the cathode operation exceeded 28,000 hours. In a gridded ion thruster, the NSTAR flight-spare thruster cathode operated for over 30,000 hours in tests run at JPL, and the test was stopped without determining the ultimate life of the hollow cathode. This endurance is impressive and exceeds almost all demands on a hollow cathode for solar electric propulsion missions. However, on proposed nuclear electric propulsion missions, thrusters will be required to operate for more than 10 years. Because of this need, we have begun a systematic investigation to understand the processes that can cause hollow cathode performance degradation and failure. This paper will present our present understanding of the hollow cathode barium depletion mechanism and the design required to achieve the required life. The models of the cathode life are based on extensive traveling wave tube impregnated cathode data in the literature, and this data is extended to the hollow cathodes used in ion thrusters. We show that the observed space station cathode life is in agreement with published barium evaporation rates for the vacuum cathodes, indicating that the cathode plasma does not significantly effect on the insert barium depletion rate. Experiments on probing the plasma characteristics in the hollow cathode using ultra-fast scanning probes and directly measuring the surface temperature of the insert by scanning fiber-optic probes provide data for the plasma models that are used to predict the cathode tempearature that ultimately determines the life.

Nomenclature

A	=	adatom sublimation coefficient
E_{eff}	=	activation energy for adatom evaporation
E_o	=	activation energy for barium evaporation
K_o	=	barium sublimation coefficient
n_o	=	particle density on the insert surface
J_D	=	discharge current
J_{total}	=	flux of material from cathode surface
J_{pl}	=	plasma ion flux to cathode surface
L_c	=	insert length
$m_{profile}$	=	slope of the insert temperature gradient
p_{insert}	=	reservoir insert porosity
r_c	=	reservoir cathode radius

[*] Principal Scientist, Advanced Propulsion Technology Group, Senior Member AIAA
[†] Group Supervisor, Advanced Propulsion Technology Group, Senior Member AIAA
[‡‡] Principal Scientist, Advanced Propulsion Technology Group, Senior Member AIAA
[§] Member Technical Staff, Advanced Propulsion Technology Group, Member AIAA.
[**] Graduate Student, Academic Part Time Staff, Advanced Propulsion Technology Group, Member AIAA
[††] Graduate Student, Summer Intern, Advanced Propulsion Technology Group

T = insert surface temperature
τ = operating time of insert
$\tau_{100\mu m}$ = time to deplete 100 mm of insert
y = insert thickness
$y_{100\mu m}$ = reference depletion thickness
y_{res} = reservoir thickness
Y_{ad} = adatom production yield
Y_{ps} = sputtered particle yield
V = reservoir volume
W = instantaneous depletion front velocity

I. Introduction

Hollow cathodes have been studied extensively since the early 1930's due to their wide range of applicability in vacuum electronic devices, microwave tubes, thyratron switches, lasers and materials processing ion sources. Over the past decade, hollow cathodes have also become a critical component in many flight electric propulsion systems such as ion propulsion and Hall-effect thrusters. Extended operation of hollow cathodes for space applications was achieved during the International Space Station (ISS) plasma contactor test at the NASA Glenn Research Center (GRC)[1] and during the Extended Life Test of the NASA Solar Electric Propulsion Technology Applications Readiness (NSTAR) engine at the Jet Propulsion Laboratory (JPL).[2] After 28,000 hrs of operation, the ISS contactor failed to restart; upon conclusion of the NSTAR ELT the main discharge chamber and neutralizer cathodes had been operating without problems after 30,352 hrs. Hollow cathode lifetimes in excess of 80,000 hrs are required for long duration missions proposed under NASA's Project Prometheus such as the Jupiter Icy Moons Orbiter (JIMO). For the proposed JIMO mission it would not be feasible to conclude life tests of such duration *and* flight qualify the system before the earliest launch date proposed for 2015. To address this lifetime requirement, a focused effort has been underway at JPL that combines theoretical modeling and experiments to quantify the plasma environment in these devices. The ultimate goal is to identify the mechanisms that cause performance degradation and failure at the required operating levels such that the life and throughput of the ion engines can be accurately predicted.

Cathodes made of porous tungsten inserts that are impregnated with barium aluminates (called dispenser cathodes) have been used in hollow cathode geometries for many years in electric propulsion devices, and are the main candidate to meet the performance and lifetime requirements for JIMO and other long missions proposed by NASA. Empirical studies of impregnated cathodes in diodes and traveling-wave tubes, carried out in the late 1970's by Palluel and Schroff[3] showed that lifetime is largely determined by the rate at which the impregnate material is depleted. Barium depletion is still considered a fundamental failure mechanism of ion thrusters, largely due to the fact that it cannot be predicted accurately to date. The rate at which barium evaporates from the surface of the porous insert in the Palluel and Schroff study was found decrease as a function of the square root of the operation time due to diffusion of the impregnate through the large aspect-ratio pores of the insert to the surface. More importantly, the measured depletion depths after operation for a given time showed a marked dependence on the cathode operating temperature. For example, after 2500 hrs of operation the barium depleted depth in an S-type cathode was found to be about a factor of three higher when the cathode temperature was 1230 ˚C compared to 1035 ˚C. This behavior leads to the "rule-of-thumb" scaling that the cathode insert life decreased a factor of 2 for about every 40 degrees of operating temperature increase. The same trend was observed under a variety of operating conditions and different cathode impregnated types that use barium/calcium aluminates.

There is a wealth of life test data on barium impregnated porous tungsten cathodes in vacuum tubes. The TriService/NASA Cathode Life Test Facility has operated a wide variety of cathodes for very long durations; some for more than 130,000 hrs (15 years!). Both reservoir and impregnated insert cathodes have demonstrated life in excess of that needed for proposed Project Prometheus missions, as illustrated in Figure 1. An intensive research effort has been underway to tap into the vacuum-device experience by relating the barium depletion rates in a plasma-filled hollow cathode with the vacuum cathode depletion rate database.

To achieve this goal, it is necessary to determine the plasma environment seen by the barium impregnated emitter surface, and to relate the effect of that environment on the barium loss rate from the surface compared to the vacuum data. First, an experimental program was undertaken at JPL to measure the plasma parameters inside a hollow cathode[4] operating at discharge currents, voltages and flow rates near that required for Project Prometheus ion thrusters. This program used miniature Langmuir probes mounted on high-speed pneumatic translational stages to measure the variation of plasma temperatures, densities, and potentials along the axis of the hollow cathode. The

axial profiles both internal to the cathode and in the plume downstream of the cathode were measured. This data is used to benchmark modeling efforts aimed at predicting the ion flux and energy at the insert surface that might affect the barium evaporation rate.

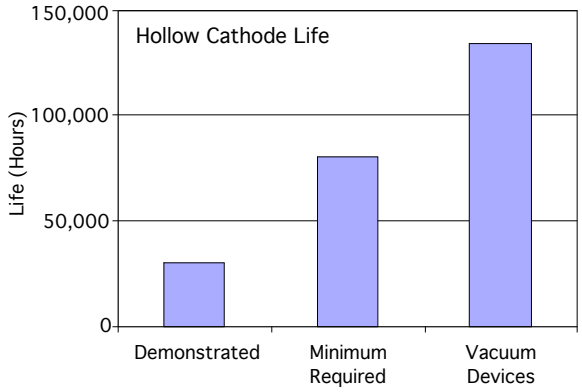

Figure 1. Vacuum-device dispenser cathodes have demonstrated operating life in excess of requirements for proposed Project Prometheus missions.

A 2-D axis-symmetric model of the neutral gas and plasma processes internal to the cathode was then developed[5]. The model was validated using the on-axis probe measurements, and was used to calculate the sheath potentials and ion and electron fluxes to the off-axis impregnated emitter surface. One major finding was that less than half of the applied discharge voltage was dropped in the sheath potential above the emitter due to the potential distribution in the plasma outside the cathode and collisional effects inside the hollow cathode plasma. As a result, the ions that strike the emitter surface were found to have a kinetic energy less than about 10 eV.

To determine the affect of this low energy ion bombardment on the barium loss rate from the surface, an experimental and theoretical effort[6] was started at the University of California, San Diego, to determine the barium evaporation rate from an impregnated cathode surface as a function of ion flux and ion energy. The experiments showed that while a flux of 25 to 30 eV ions increases the effective barium evaporation rate from the porous tungsten surface by an order of magnitude, ions with less than 10 eV, as predicted by the model, made no change to the evaporation rate compared to thermally induced evaporation. These results agreed with an adatom model[7] developed at UCSD that has been used to successfully predict the enhanced evaporation of other liquid metals on surfaces exposed to plasma bombardment. As a result, the barium evaporation rate from the emitter surface inside the xenon hollow cathode plasma is determined solely by thermal evaporation, and therefore is the same as for a similar cathode operating in vacuum.

Since the barium evaporation rate in the hollow cathode depends only on the surface temperature, it is possible to calculate the barium depletion-limited life in a hollow cathode based on vacuum-cathode results if the emitter operating temperature is known. This is the same critical piece of data used to determine vacuum cathode life. Measurements of emitter surface temperature in an operating hollow cathode have been made using two-temperature pyrometry[8]. These experiments have shown insert temperatures of a Space Station Plasma Contactor-size cathode operating at full current to be in excess of about 1200 ˚C and have a small gradient along the length of the insert.

Finally, an estimate of cathode life from barium depletion has been developed based on Paullel's measurements of barium depletion depth as a function of time and the insert temperature. The model is benchmarked to the temperature measurements made on the SSC cathode, and applied to the larger cathodes anticipated to be needed for JIMO-sized thrusters such as NEXIS[9][10]. The model predicts a life for the NEXIS cathode consistent with that required for JIMO, and suggests ways of extending the cathode life as required for other classes of missions.

II. Experimental Investigation of Hollow Cathode Plasma Parameters

The detailed study[4] of the plasma structure inside operating hollow cathodes uses a pneumatically driven scanning probe diagnostic shown in the photograph in Figure 2. This device rapidly inserts a miniature probe directly through the insert region and into the hollow cathode orifice from the upstream insert region inside the hollow cathode to produce complete axial profiles of the plasma density, temperature and potential. A similar pneumatic probe is scanned from the anode region through the keeper into the cathode orifice to provide similar axial profiles outside the cathode, but this data is not required for the work reported here. The cathode probe is extremely small to avoid perturbing the plasma; the ceramic tube insulator is 0.5mm in diameter with a probe tip area of 0.002 cm^2. The probe is scanned through the plasma at speeds of over 1mm/msec to avoid melting, and resides in the high plasma density orifice region for only about 10 msec. At discharge currents of 10 to 25 A, the plasma density in the insert region is found to exceed 10^{14} cm^{-3}, with the peak density occurring upstream of the orifice. Figure 3 shows examples of the xenon plasma density profile from the cathode-scanning probe in a 25 A discharge for two different cathode flow rates.

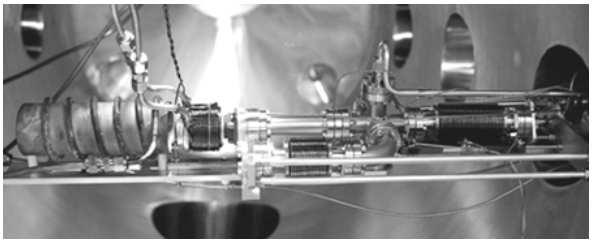

Figure 2. Photograph of the pneumatic scanning probe assembly with the cathode in the center and a cylindrical anode on the left.

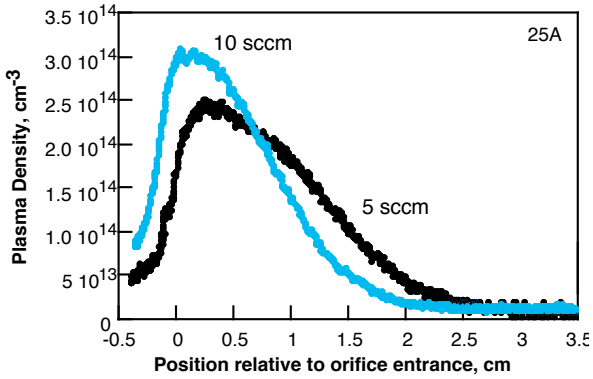

Figure 3. Plasma density scans from the cathode probe at 25 A for two cathode flow rates (from ref. 4).

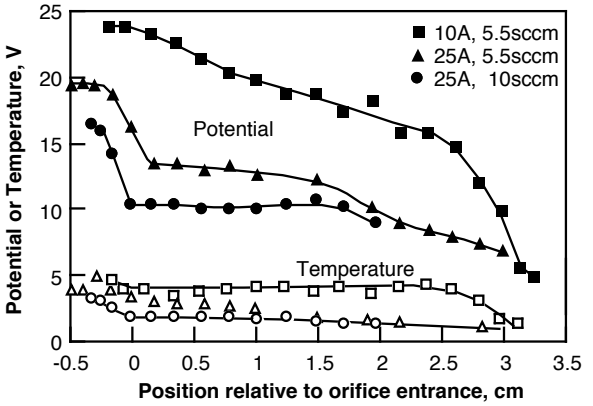

Figure 4. Plasma potential and electron temperature profiles in the hollow cathode showing variation with flow and discharge current (from ref. 4).

Plasma potential profiles on axis in the insert region are shown in Figure 4, and are found to be in the 10 to 20 V range with electron temperatures of 2 to 5 eV, depending on the discharge current and gas flow rate. The probe measurements in the insert region suggest that the electron distribution function has a depleted tail, which is likely due to the high collisionality of this plasma in the insert at the pressures in excess of 1 Torr measured in the cathode. Double layers are also observed in the orifice region, and tend to change location and magnitude with the discharge current and gas flow rates. The potential and temperature profiles inside the cathode are found to be insensitive to anode configuration changes that alter the discharge voltage at a given flow. This implies that the ion flux and bombardment energy to the cathode surface is determine by the criteria for self-heating of the cathode to emission temperatures. Application of an axial magnetic field characteristic of the cathode region of ring-cusp thrusters increases the plasma potential in the insert and orifice regions and the plasma density in the cathode plume.

III. 2-D Model of the Hollow Cathode Insert Region

A 2-D physics-based model[5] of the plasma in the hollow cathode insert region was developed to predict the xenon ion energy and flux actually striking the insert surface. The plasma in the hollow cathode insert region consists of a weakly ionized, highly collisional, multi-component fluid. Although anomalous effects are possible (as it will be shown later) the dominant mechanisms that determine the transport of charge, mass and heat in the plasma are classical collisions that occur between electrons and neutrals (e-n), electrons and ions (e-i) and, ions and neutrals (i-n). The latter is mainly due to resonant charge exchange between fast ions and slow neutrals with an associated average collision cross section in the order of 100 Å for xenon at low energies. Under the operating conditions of interest, the mean free paths associated with these particle collisions are all small compared to the hollow cathode channel size ($0.002<Kn<0.2$). Our theoretical model is therefore based on a "fluid" approach, which assumes that particles are perturbed from their Maxwellian distribution function only by virtue of collisions, and relax to their equilibrium distribution within the mean time between collisions.

The physical configuration modeled for the NEXIS cathode is shown in Figure 5. The conservation and constitutive equations, which the model is based on, assume a quasi-neutral plasma, and have been described in detail by Mikellides, *et al*.[5] The species continuity equations for electrons and ions include the effects of ionization based on collision cross sections published in the literature. The plasma inertia terms (for both electrons and ions), and the magnetic field, are neglected in the conservation of momentum equations. However, interspecies "friction" terms as well as the pressure gradient terms for both ions and electrons are retained. Conservation of electron energy includes thermal conduction, power associated with the work done by the electric field, interspecies heat

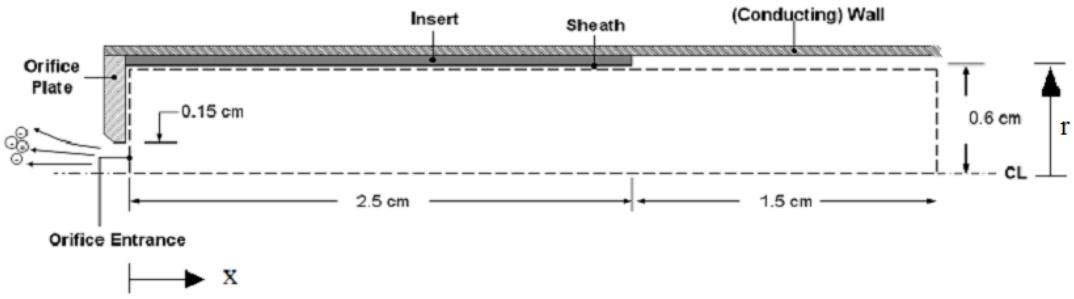

Figure 5. Physical configuration of the NEXIS hollow cathode model.

exchange as a result of elastic collisions, and inelastic energy losses by ionization. The heavy species - ions and neutrals - are assumed to be in thermal equilibrium; the expression representing their energy conservation also includes thermal conduction and heat exchange from ion-neutral collisions. It is in fact found that the latter is the dominant term for the heating of the neutral gas in the hollow cathode to temperatures as high as 2800 ^{o}K.

The emitted electron current density from the insert wall is implemented as a condition along the insert boundary and is modeled after the Richardson-Dushman equation for thermionic emission. The sheath at all walls is assumed to act as a perfect thermal insulator. The Richardson-Dushman condition requires an effective insert temperature profile, which in the present model is specified to match the measured temperature profile[5] of the insert in a 6.4-mm (outer channel) diameter cathode operated at a discharge current of 12 A. In the simulations presented here, the peak insert temperature is varied until the value of the total current through the orifice matches the operating current of the case under investigation (specifically 25 A of discharge current). At the cathode orifice the boundary conditions for the plasma density and potential are fixed based on the probe data discussed above. The conservation equations are discretized using a finite volume approach. The iterative approach to solve numerically the complete system of equations completes the modeling.

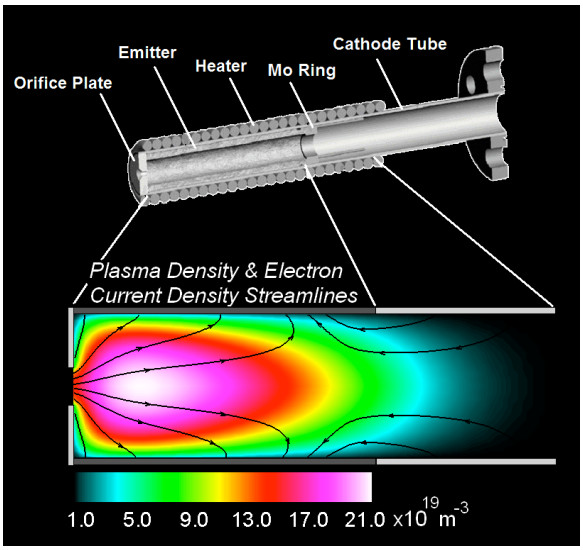

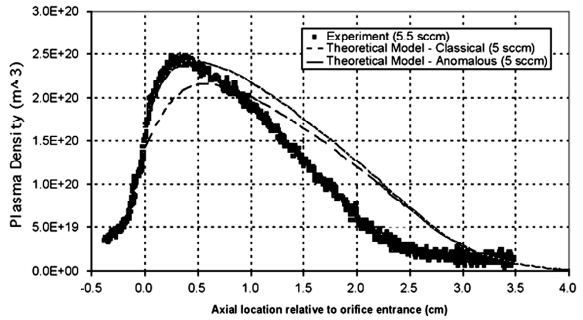

Figure 7. Comparison between two modeling results and measurements taken at a discharge current of 25A (from ref. 5).

Figure 6 shows the computed plasma density overlaid by electron current density "streamlines." Immediately apparent is a non-monotonic behavior exhibited by the plasma density along the hollow cathode channel, which is contrary to previous experimental observations in lower current, smaller size cathodes.[11,12] The theoretical results are supported by experimental observations recently obtained at JPL in a NEXIS cathode[9,10]. It is suggested that the non-monotonic behavior is mainly due to the larger channel size of the high-current cathode and the larger open area of the orifice that allows sufficiently high rates of gas and plasma flow out of the cathode. Moreover, since plasma is also lost into the orifice plate through the sheath, the larger orifice plate area also enhances the rate of plasma loss from the cathode.

A comparison with of the plasma density data with the model predictions, computed at the centerline as a function of distance from the orifice entrance, is shown in Figure 7. The measured profile in Fig. 7 was obtained at a discharge current of 25 A and a gas flow rate of 5.5 sccm. Additional comparisons are shown in Figure 8 for the plasma potential and electron temperature. The calculations and comparisons with the experimental data suggest that far upstream of the orifice (z>2cm), mass and heat transport occur classically. Closer to the orifice however, the measurements provide good agreement if anomalous resistivity is included. Our investigation suggests that

anomalous heating in this region may occur as a result of two-stream instabilities,[13] which may be accounted for using a phenomenological model for anomalous resistivity.[14] The benchmarked model agrees well with the experimental data.

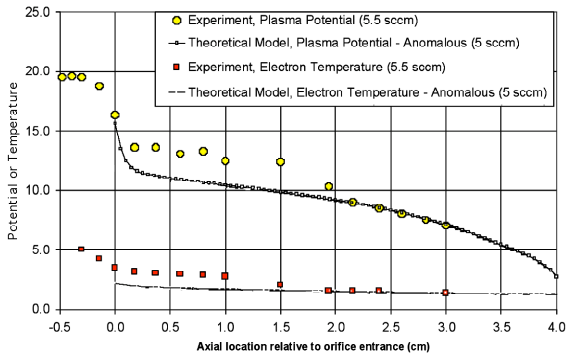

Figure 8. Comparison between model results and measurements for the plasma potential and electron temperature at discharge current of 25 A.

A number of conclusions may be drawn from the model results and comparisons with the recent data obtained at JPL. The model suggests that the dominant heating mechanism of the neutral gas is resonant charge-exchange collisions between fast ions and slow neutrals. The total emitted electron current is found to significantly exceed the discharge current, with the difference resulting from relatively energetic plasma electrons in the tail of the distribution returning to the cathode surface. Most importantly, the model predicts peak voltage drops at the emitting surface not exceeding 8 V, which is less than half of the applied discharge voltage, and ion fluxes of less than 1 A/cm^2 at the 25 A discharge currents baselined here for a NEXIS-size thruster. These ion energies and particle fluxes striking the emitter surface are used to determine the rate at which barium is removed from the surface in separate experiments performed at UCSD.

IV. Barium Removal from the Emitter Surface

The experimental and theoretical study of enhanced barium evaporation from dispenser cathode surfaces was undertaken[6] at UCSD. The experimental arrangement shown in Figure 9 (from ref. 6) was used to measure the barium evaporation from a Type-B 411 impregnated porous tungsten cathode with an embedded heater during xenon plasma bombardment. The planar cylindrical cathode was heated by a DC power supply and inserted into the center of the plasma chamber at a distance of approximately 25 cm downstream of the plasma source exit plane. The sample temperature was measured with both optical pyrometry as well as via a thermocouple clamped to the side of the cathode assembly. The cathode could also be biased negatively relative to the plasma in order to control the ion bombardment energy. Finally, an optical fiber assembly collected light along a line-integrated chord that traverses the center of the plasma, and then transmitted this light to a visible wavelength spectrometer which records the relative emission intensity of Ba-I line emission at 553.5 nm in the plasma. Since the emission intensity depends not only upon the amount of Ba present in the plasma, but also upon the electron density and temperature, the Ba-I signal was normalized to the neutral xenon line to account for any variations in plasma parameters during the measurements. In all cases reported here, such variations were found to be much smaller than the observed large variations in Ba emission intensity.

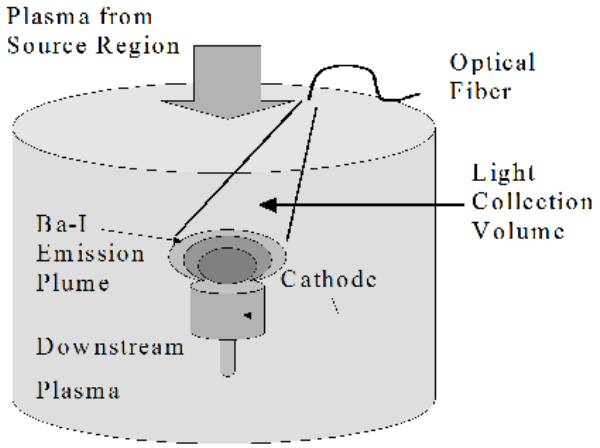

Figure 9. Schematic of Ba cathode emissivity measurement geometry showing the plasma source above and the dispenser cathode (from ref. 6).

The variation of Ba emission with surface temperature and/or with ion bombardment energy was measured for xenon ion fluxes of <10^{18}cm^{-2}. Figure 10 shows the barium loss rate at 725 ˚C versus the ion bombardment energy. We see that increasing the ion bombardment energy from 10 to 30 eV increases the barium loss rate by an order of magnitude. Figure 11 shows the barium loss rate as a function of temperature for two cathode bias energies. For the case of the cathode floating relative to the plasma, the ion bombardment energy is only a few eV and the barium loss rate is determined solely by thermal evaporation. For a bias energy of 15 eV, the barium loss rate is found to be the same as for thermal evaporation for cathode

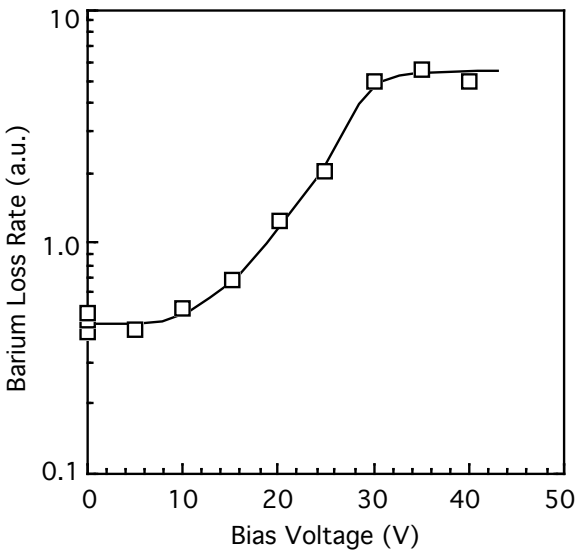

Figure 10. Variation of barium loss rate from the cathode surface at 725 ˚C with cathode bias voltage (from ref. 6).

temperatures in excess of about 800 ˚C. Since the hollow cathodes in JIMO-size thrusters operate at insert temperatures in excess of 1000 ˚C, this data shows that the barium loss rate is determined by thermal evaporation rates.

A model of the enhancement of barium evaporation for a surface under energetic ion bombardment was developed to explain this behavior. At elevated surface temperatures, two classes of surface particles must be considered at the surface: (a) those particles that are bound to the material lattice structure (denoted here as "lattice atoms"), and (b) atoms that have been liberated from the lattice structure, but which as still bound to the material surface with a reduced binding energy (denoted here as "adatoms"). Both species can sublimate from the material surface if an atom receives enough kinetic energy from random collisions to break free from the surface; however because the binding energy for the two species is different, the corresponding loss rate will also be different.

The net flux of material from the surface can be written as

$$J_{Total} = J_{pl} Y_{ps} + K_o n_o \exp^{(-E_o / T)} + \frac{Y_{ad} J_{pl}}{\left(1 + A \exp^{(E_{eff} / T)}\right)} \quad (1)$$

where J_{pl} is the plasma ion flux and Y_{ad} is the adatom production yield from the incident ion flux, Y_{ps} is the sputtered particle yield, $Y_{ad}J_{ipl}$ is equal to the adatom loss rate due to both sublimation and recombination.

The first term describes physical sputtering of lattice atoms (which is independent of surface temperature), the

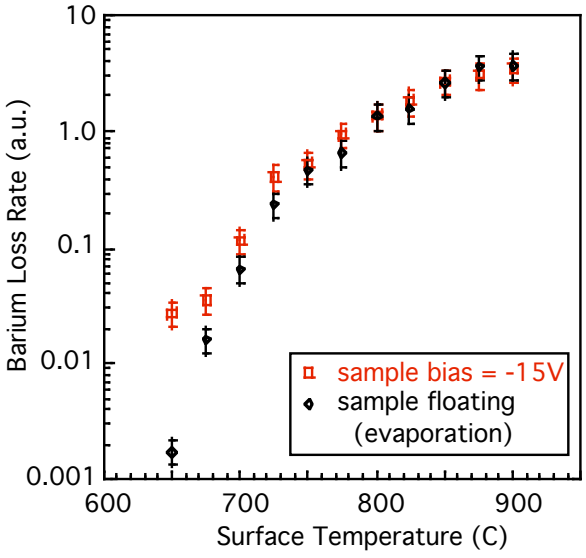

Figure 11. Relative Ba concentration in Xe plasma for a –15V cathode bias and a floating cathode exhibiting thermal evaporation (from ref. 6).

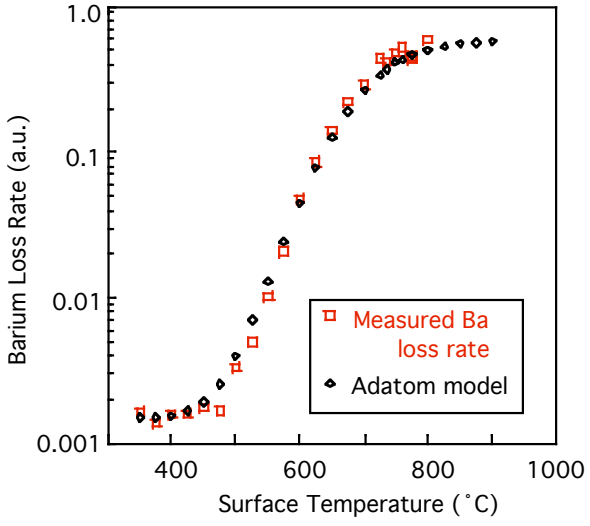

Figure 12. Ba concentration versus cathode surface temperature for 30 V cathode bias. Experimental data are shown by open squares and the model prediction with Y_{ps}~0.002

second term describes the thermal sublimation of lattice atoms, which is independent of ion flux, and the third term describes the losses due to adatom production and subsequent sublimation, which depends upon both the incident ion flux and the surface temperature. For Xe ions incident on BaO at 30 eV, Yps=0.02, A=2x10^{-9} and

$$\frac{Y_{ad}}{Y_{ps}} \approx 400 \tag{2}$$

We have used these parameters to model the expected net flux of Ba from a surface under bombardment with 30 eV Xe ions for various surface temperatures. The result of this model is compared with experimental measurements of Ba emissivity under these conditions in Figure 12. The model compares extremely well with the experimental results. The model can also qualitatively explain the key experimental observations, including the effect of ion energy on net erosion, the saturation of the adatom loss term at elevated temperatures, and the transition to losses dominated by thermal sublimation of lattice atoms at elevated temperatures. The model has been used to examine the effect of increasing the ion flux to the surface from the values in these experiments to the actual values for the hollow cathodes from the 2-D plasma model. In this case, the model predicts that thermal evaporation dominates the barium loss rate for ion energies of less than 15 eV and cathode temperatures of over 900 ˚C. The model provides confidence that the barium loss rate effects in the plasma are understood, and that the main results of barium loss determined by thermal evaporation rates for the parameters of the JIMO-class cathodes examined here are accurate.

V. Cathode Insert Temperature

Since the barium evaporation rate for the plasma conditions found in the hollow cathodes are determined by the insert surface temperature, a non-contact temperature measurement technique was developed[8] to directly measure the insert temperature during cathode operation. The technique employs a stepper-motor driven fiber optic probe that is scanned along the insert inside-diameter and collects the light radiated by the insert surface. Ratio pyrometry is used to determine the axial temperature profile of the insert from the fiber optic probe data. Thermocouples attached on the outside of the cathode on the orifice plate provide additional temperature data during operation and are used to calibrate the pyrometer system in-situ with a small oven inserted over the cathode to equilibrate the temperature. Figure 13 shows temperature profile for a nominal "1/4-inch" Space Station Contactor (SSC) cathode operating at four different discharge currents. The peak temperature of the insert at the full 12 A current level is about 1200 ˚C. The insert also has approximately a 10 to 15% temperature gradient along its' length.

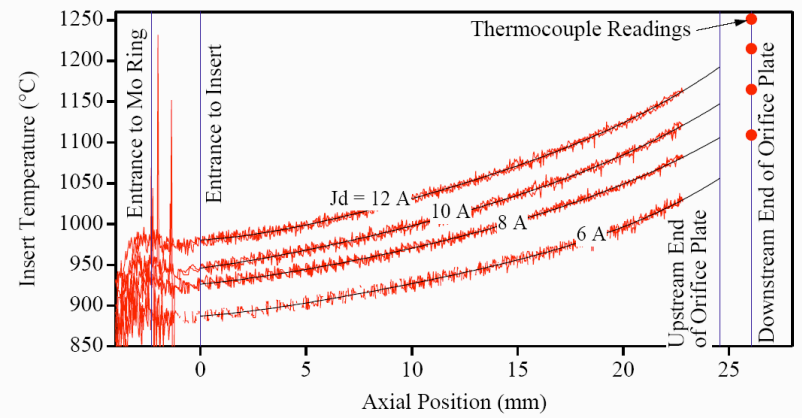

Figure 13. Insert temperature profile for a SSC hollow cathode sized system for several different discharge currents.

For the JIMO-class thruster hollow cathodes, the actual operating temperature has not yet been measured. The lifetime model for barium depletion assumes that the NEXIS cathode also possesses a similar temperature profile, with the highest temperature occurring at the cathode orifice. Regression analysis on the data in Fig. 12 indicates that the temperature profiles are nearly linear with an average slope of 7240 ˚K/m. A simple way to determine the insert temperature at points a distance x away from the cathode orifice is

$$T_{insert}(x) = T_{max} - m_{profile}\, x, \tag{3}$$

where T_{max} is the insert temperature at the orifice and $m_{profile}$ is the magnitude of the temperature profile slope (7240 ˚K/m for this data). A larger slope in the temperature away from the orifice would result in a quicker

temperature drop-off within the cathode, but this is not assumed at this time and may be corrected later as more data for larger cathodes is acquired.

The actual insert temperature at the orifice is obtained from the 2-D plasma model where the electron emission is determined from an integration of the Richardson-Dushman equation corrected for an effective Schottky field enhancement along the length of the insert with the Eq. 3 temperature gradient. The peak temperature near the orifice is then iterated until the total insert emission produces the desired discharge current exiting the cathode orifice. The model provides scaling for the peak temperature as a function of the discharge current given approximately by equation

$$T_{max} = 1370 + 3.971 \times 10^{-7} J_D^{\,6}, \tag{4}$$

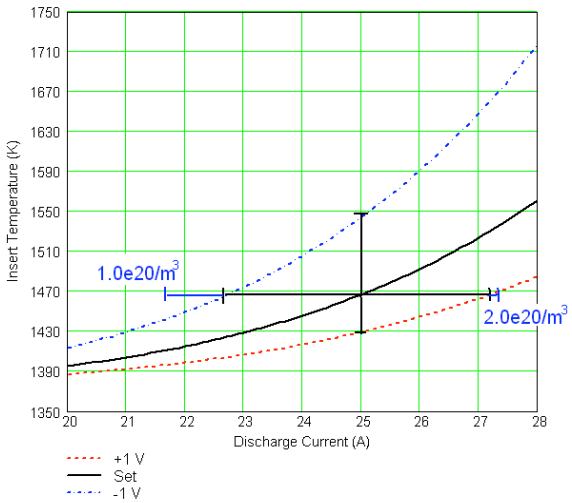

Figure 14. Maximum insert temperature dependence on the discharge current for a range of plasma potentials and densities at the orifice.

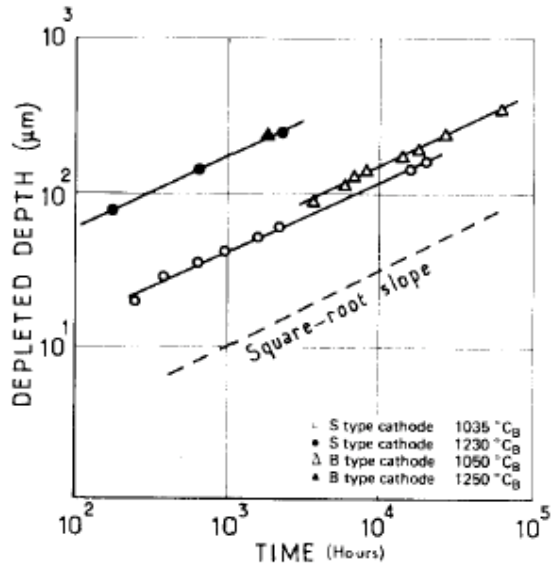

Figure 14. Depletion depth of a porous tungsten insert as a function of time for cathodes at different temperatures (from ref. 3).

where discharge current J_D is in amperes and T_{max} is the temperature in Kelvin.

It should be noted that this result is sensitive to the boundary conditions of the plasma at the orifice and the temperature gradient. For example, Figure 14 shows the calculated peak insert temperature from the model as a function of the calculated discharge current which produced Eq. 4. Also shown of the plot is the effect of varying the plasma potential and plasma density boundary conditions at the orifice entrance in the model. We see that a ±1 V change in the plasma potential from the measured values changes the peak temperature by about 10%. A change in the plasma density by a factor of 2 at the orifice plate also changes the discharge current calculated by 16%. While the present results are based on the probe measurements, additional modeling to predict these boundary conditions and measurements of the actual temperature of NEXIS cathodes will enhance the accuracy of the results.

VI. Barium Depletion Model

The previous sections showed that the barium loss rate from hollow cathode impregnated inserts should be essentially unchanged from the same inserts operated in vacuum. Published measurements by Palleul and Shroff[3] of the depth of barium depletion in dispenser cathodes as a function of time and temperature show that barium depletion obeys a simple diffusion law with an Arrhenius dependence on temperature. This is shown in Figure 14 (from ref. 3), where the impregnate surface layer in the pore recedes with time. The "activation energy" in the diffusion coefficient that determines the slope of the curves in Fig. 14 appears to be relatively independent of the cathode type.

This data has been applied to the life-test results from the Space Station Contactor cathode using the insert temperature measurements on this size cathode that were shown in Fig. 13. This cathode has an insert thickness of about 760 μm. The orifice plate temperature measured with a thermal couple is 1250º C, while the extrapolated temperature based on the optical measurements is about 1200º C. Using these two temperatures, the depletion time for the downstream edge of the insert is in the range of 20,000 to 40,000

hours, a range that brackets the measured life of 28,000 hours[1].

The linear relation in the semi-log plot of Fig. 14 can be represented by

$$\log \tau(x) = 1.4257 \frac{10^4}{T(x)} - 6.7327 , \tag{5}$$

where the operating time $\tau(x)$ is in hours and $T(x)$ is in Kelvin, and x is the position along the length of the cathode insert. The depth of the depleted layer is found to be proportional to the square root of the operating time[3]. The relationship between insert depletion depth and operating time (normalizing to the case of a 100-micron depletion depth from the literature[3]) yields a cathode life of

$$\tau_{life} = \tau_{100\mu m} \left(\frac{y}{y_{100\mu m}} \right)^2 , \tag{6}$$

where $\tau_{100\mu m}$ is the time to deplete to 100 μm in depth, y is the insert thickness, and $y_{100\mu m}$ is the 100 μm reference depth.

Using Eq. 6 and the performance of the NEXIS ion thruster[9,10], it is possible to estimate the life of the dispensor hollow cathode based on barium depletion. The Laboratory Model NEXIS thruster operates at 75 to 78% efficiency over an Isp of 6000 to 8000 sec. The existing insert has a thickness (depth) of about 1.5 mm and an insert length of about 2.5 cm. Figure 15 shows the model predicted depletion limited life of this insert versus specific impulse for several thruster power levels. At the nominal operating point of 7000 sec Isp and 20 kW, the cathode is projected to operate for about 100,000 hours. Increasing the Isp requires operation at higher beam voltages, which for a given power requires less beam current and thereby less discharge current. A lower discharge current reduces the insert temperature for a given cathode size, which reduces the barium evaporation rate and extends the cathode life. Likewise, lower Isp's and higher power require higher discharge currents, which translates in a reduction in the cathode life. It should be noted that the cathode life in Eq. 6 goes as the insert thickness squared, so the life at any operating point in Fig. 15 can be extended simply by increasing the thickness of the insert. This may require increases in other dimensions in the cathode like the outside diameter or orifice size, but proper selection of these dimensions will maintain the insert temperature at a reasonable level to provide the desired life.

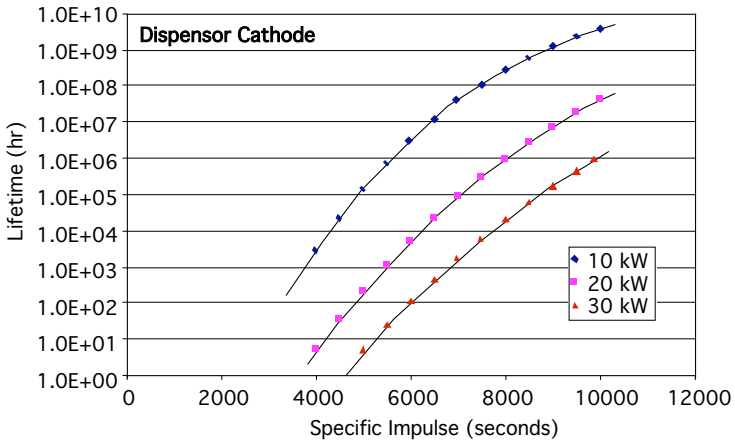

Figure 15. Model prediction of NEXIS dispensor cathode life versus Isp for several thruster powers.

VII. Reservoir Cathode Life

The reservoir cathode uses a porous tungsten layer with an enclosed volume behind the layer in which large quantities of the barium/aluminate impregnate is stored. This geometry has the capability of providing more barium than a given dispensor cathode because the reservoir size is larger than the pore volume. Reservoir cathodes have been life tested as a part of the TriService/NASA Cathode Life Test Facility experiments mentioned earlier, and demonstrated stable operation and life of over 100,000 hours. A reservoir hollow cathode was developed at JPL[15], and is in test for use in NEXIS.

The reservoir cathode has a barium transport in the pores that is diffusion limited, similar to dispenser cathodes, and so Eq. 6 still applies. The depletion layer in this case will recede with the instantaneous depletion velocity at each point *x* along the reservoir-insert interface being

$$W(x) = \frac{d\,y_{res}}{dt} = \frac{1}{2}\left(\frac{y_{100\,\mu m}}{y_{res}}\right)\left(\frac{y_{100\,\mu m}}{\tau_{100\,\mu m}(x)}\right). \tag{7}$$

This depletion velocity is assumed to remain steady with time, implying that the reservoir-insert interface does not change during cathode operation. Along the cathode, the depletion velocity is a maximum close to the cathode orifice and decreases with axial distance away from the orifice due to the temperature gradient in the cathode. Thus in the axial direction, a barium concentration gradient builds up in the reservoir that can result in axial barium diffusion.

Two limiting cases exist for this axial barium diffusion in the reservoir. The fast diffusion case assumes that the axial diffusion rate is sufficiently fast such that that it is able to replenish each point along the reservoir-insert interface at the same rate as the barium is being depleted. If so, the cathode fails upon exhaustion of all available barium in the reservoir, and this depletion time τ_{life} is given by

$$\tau_{life} = \frac{V}{\int_0^{L_C} W(x)\, 2\pi r_C\, dx}, \tag{8}$$

where L_C is the insert length and V_{Ba} is the effective reservoir volume. An effective reservoir volume is needed because the operating time used in Eq. 8 is intended for barium depletion in a porous tungsten matrix. Since the composition of the reservoir source material is assumed to be similar to that of the impregnates within the pores of impregnated cathode inserts, the effective reservoir volume is related to the actual reservoir volume V_{res} and the insert porosity p_{insert} by

$$V = \frac{V_{res}}{p_{insert}}. \tag{9}$$

The above case provides for an optimistic estimate of the barium depletion lifetime. However, if the axial barium diffusion rate is not sufficiently fast, then the insert region by the cathode orifice would be the fastest region to exhaust its barium supply. In this limit, which provides for the most conservative estimate of barium depletion time, the axial barium diffusion rate is negligible. Consequently, the depletion time as determined by the orifice region is

$$\tau_{life} = \frac{t_{Ba}}{W(0)}, \tag{10}$$

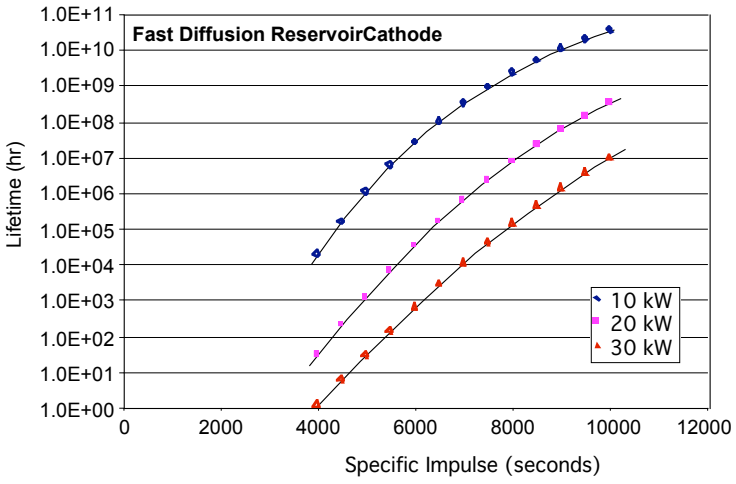

Figure 16. Reservoir cathode life using the fast axial diffusion model versus Isp for several NEXIS thruster power levels.

where the effective barium layer thickness t_{Ba} is defined as

$$t_{Ba} = \frac{V}{2\pi r_C L_C}. \tag{11}$$

The present reservoir cathode[15] life using the fast diffusion model is shown in Figure 16. In this case, the cathode life is significantly longer than the dispensor cathode of Fig. 15 due to the increased volume of impregnate available. This is the upper limit for life of this particular cathode design, although versions with larger reservoir volumes could be designed to further extend the cathode life.

VIII. Conclusions

A focused program has been undertaken to predict the hollow cathode life for deep space missions using physics models benchmarked by detailed experimental data. This effort required the development of a 2-D plasma model inside the hollow cathode that was benchmarked by non-perturbing probe measurements in the operating cathode to predict the xenon ion energy and flux striking an impregnated dispenser cathode insert. A separate set of experiments at UCSD concluded that the barium loss rate under the conditions inside the NEXIS hollow cathode was determined by thermal evaporation and was not enhanced by the plasma bombardment, meaning that the cathode life could be modeled using vacuum cathode physics. Measurements of the insert temperature inside a smaller hollow cathode provided information used to estimate the NEXIS cathode temperature, which provided the barium depletion time for a given cathode insert size from the cathode physics models. The temperature and the vacuum cathode depletion physics were used in a simple model to estimate the cathode life for both dispenser and reservoir cathodes operating in a JIMO-class thruster.

This paper represents the first non-empirical effort to produce a hollow cathode life model using plasma-physics and vacuum-cathode-physics models benchmarked by specific experimental measurements. The large sensitivity of the barium diffusion and evaporation rates to the actual insert surface temperature during operation causes factors of up to 2 uncertainty in the present predictions. Additional measurements of the actual NEXIS cathode temperature planned for the near future, coupled with improvements in the plasma modeling inside the cathode, will greatly increase the accuracy of these predictions. It is anticipated that the on-going cathode development efforts for Project Prometheus and the accumulated wear test data from these cathodes in the coming years will also contribute to improving the accuracy and confidence in this model.

Acknowledgments

The research described in this paper was carried out by the Jet Propulsion Laboratory, California Institute of Technology, under a contract with the National Aeronautics and Space Administration in support of Project Prometheus.

References

[1] Sarver-Verhey, T.R., "28,000 Hour Xenon Hollow Cathode Life Test," IEPC Paper 97-168, November 1997.

[2] Sengupta, A., Brophy, J. R., Goodfellow, K. D." Status Of The Extended Life Test Of The Deep Space 1 Flight Spare Ion Engine After 30,352 Hours of Operation", AIAA Paper 03-4558, July 2003.

[3] Palluel, P., and Shroff, A.M., "Experimental Study of Impregnated-Cathode Behavior, Emission, and Life," Journal of Applied Physics, Vol. 51, No. 5, 1980, pp. 2894-2902.

[4] D.M. Goebel, K. Jameson , R. Watkins, I. Katz, "Hollow Cathode and Keeper-Region Plasma Measurements Using Ultra-Fast Miniature Scanning Probes", AIAA-2004-3430, July 2004.

[5] Mikellides, I., Katz, I., Goebel, D. and Polk, J., "Theoretical Model of a Hollow Cathode Insert Plasma," AIAA Paper 04-3817, July 2004.

[6] R. Doerner, G.R. Tynan, E. Oyerzabal, K Taylor, D.M. Goebel, I. Katz, "Plasma Surface Interaction Studies for Next-Generation Ion Thrusters" AIAA-2004-4104, July 2004.

[7] R.D. Doerner, et al., J. Appl. Phys. 95 (2004) 4471

[8] Polk, J., Marrese, C., Thornber, B., Dang, L., and Johnson, L., "Temperature Distributions in Hollow Cathode Emitters," AIAA Paper 04-4116, July 2004.

[9] J. Polk, et al., "An Overview of the Nuclear Electric Xenon Ion System (NEXIS) Program", AIAA-2003-4713, 40th AIAA Joint Propulsion Conference, Fort Lauderdale, FL, July 11-14, 2004.

[10] T. Randolph and J. Polk, "An Overview of the Nuclear Electric Xenon Ion System (NEXIS) Activity", AIAA-2004-3450, 40th AIAA Joint Propulsion Conference, Fort Lauderdale, FL, July 11-14, 2004.

[11] Siegfried, D.E., and Wilbur, P.J., "An Investigation of Mercury Hollow Cathode Phenomena," AIAA Paper 78-705, April 1978

[12] Domonkos, M.T., Gallimore, A.D., Williams, G.J., Patterson, M.J., AIAA Paper 99-2572, June 1999.

[13] Stringer, T.E., "Electrostatic Instabilities in Current-Carrying and Counterstreaming Plasmas," Plasma Physics, J. Nucl. Energy, Part C, Vol. 6, 1964, pp. 267-269.

[14] Sagdeev, R.Z., Proceedings of the 18th Symposium in Applied Mathematics, 1967 (unpublished) p. 281.

[15] J. Polk, "Reservoir Cathode for High Power Ion Thrusters", AIAA-2004-3970, July 2004.